ISSN 1063-7745, Crystallography Reports, 2014, Vol. 59, No. 6, pp. 867–873. © Pleiades Publishing, Inc., 2014.
Original Russian Text © R.K. Rastsvetaeva, S.M. Aksenov, N.V. Chukanov, I.S. Lykova, I.A. Verin, 2014, published in Kristallografiya, 2014, Vol. 59, No. 6, pp. 955–961.

STRUCTURE OF INORGANIC COMPOUNDS

Dedicated to the International Year of Crystallography

Iron-Rich Schüllerite from Kahlenberg (Eifel, Germany): Crystal Structure and Relation to Lamprophyllite-Group Minerals

R. K. Rastsvetaeva[a], S. M. Aksenov[a], N. V. Chukanov[b], I. S. Lykova[c], and I. A. Verin[a]

[a] *Shubnikov Institute of Crystallography, Russian Academy of Sciences, Leninskii pr. 59, Moscow, 119333 Russia*
e-mail: rast@ns.crys.ras.ru
[b] *Institute of Problems of Chemical Physics, Russian Academy of Sciences, Chernogolovka, Moscow oblast, 142432 Russia*
[c] *Moscow State University, Moscow, 119992 Russia*

Received December 25, 2013

Abstract—A single-crystal sample of iron-rich schüllerite found at the Kahlenberg quarry in the Eifel paleovolcanic field (Germany) was studied by X-ray diffraction. The triclinic unit-cell parameters are as follows: $a = 5.4061(1)$ Å, $b = 7.0416(6)$ Å, $c = 10.2077(7)$ Å, $\alpha = 99.86(1)°$, $\beta = 97.8(1)°$, and $\gamma = 89.98(1)°$. The structure was solved by direct methods in sp. gr. $P1$ and refined to the R factor of 7.9% based on 4321 $|F| > 6\sigma(F)$. The idealized formula is $Ba_2Na(Ca,Mn)(Fe^{2+},Fe^{3+})MgTi_2[Si_2O_7]_2O_2(O,F)F$. The new mineral differs from schüllerite by a lower sodium content and higher iron and calcium contents and is characterized by some distinguishing structural features. The dependence of the topology of layered *HOH* modules on the sodium content in schüllerite and lamprophyllite-group minerals and the character of regular intergrowths of these minerals are discussed.

DOI: 10.1134/S1063774514060248

INTRODUCTION

The representative heterophyllosilicate family [1, 2] includes, in particular, the lamprophyllite group comprising 11 mineral species and their varieties. The structures of lamprophyllite-group minerals are based on three-layer *HOH* modules (*H* means hetero; *O* means octahedra) consisting of a cation layer composed of edge-sharing octahedra and an anion network formed by Si diortho groups, which are most often linked together by Ti semioctahedra (unlike most other titanium heterophyllosilicates, in which titanium is in octahedral coordination). Large Sr, Ba, and K cations are located between the three-layer modules. Barytolamprophyllite and its Ba,Na-ordered analogue nabalamprophyllite, as well as lileyite, emmerichite, and ericssonite, are Ba-dominant representatives of the lamprophyllite group. Yet another barium-rich mineral schüllerite found recently at the Lohley basalt quarry (Germany) [3, 4] is characterized by chemical and structural features that distinguish it from other lamprophyllite-group minerals.

In the present work, we studied schüllerite from another locality by X-ray diffraction. The mineral was found in the late pneumatolithic association with alkali basalt at the Kahlenberg quarry in the Eifel paleovolcanic field (Germany). In this locality, schüllerite forms brown thin-plate crystals in association with nepheline, augite, fluorapatite, perovskite, magnetite, and altered götzenite. Nine heterophyllosilicate samples from Kahlenberg were studied by electron microprobe analysis. Two of them proved to be lileyite, six samples were found to be schüllerite occurring in epitaxial intergrowths with lileyite, and one sample was pure schüllerite. The crystal of the latter was used to study the structure.

EXPERIMENTAL AND STRUCTURE REFINEMENT

The chemical composition of the sample was determined from electron microprobe analysis, which was carried out using a VEGA TS 5130MM SEM scanning electron microscope coupled with an energy-dispersive X-ray spectrometer and equipped with an INCA Si(Li) detector operating at 20 kV and a probe current of 0.6 nA. This composition can be described by the empirical formula ($Z = 1$) $Ba_{1.7}Sr_{0.2}K_{0.1}Na_{0.85}Mg_{0.6}Mn_{0.5}Ca_{0.55}Fe_{1.8}Ti_{1.4}Al_{0.2}Nb_{0.1}Si_4O_{17}F$. The valence state of iron was not determined because there was an insufficient amount of the substance. The sample from Kahlenberg differs from holotype schüllerite [4] in that it has less sodium (0.85 instead of 1.05 atoms per formula unit) supplemented with calcium (0.43 instead of 0.3 atoms) and mainly a higher iron content (1.8 instead of 1.46 atoms).

The X-ray diffraction data set was collected from a flattened single crystal within a full sphere of reciprocal space on an Oxford Diffraction Xcalibur diffractometer equipped with a CCD detector. The crystallographic characteristics and the X-ray data-collection and structure-refinement statistics are given in Table 1.

Table 1. Crystallographic characteristics and X-ray-data-collection and structure-refinement statistics

Idealized formula	$Ba_2Na(Ca,Mn)(Fe^{2+},Fe^{3+})MgTi_2[Si_2O_7]_2O_2(O,F)F$
a, b, c, Å	5.4061(1), 7.0416(6), 10.2077(7)
α, β, γ, deg	99.86(1), 99.78(1), 89.98(1)
V, Å^3	377.1(1)
Crystal system, sp. gr., Z	Triclinic, $P\bar{1}$, 1
M; D_x, g/cm^3; μ, cm^{-1}	969; 4.2; 90
Crystal dimensions, mm	0.13 × 0.2 × 0.24
Diffractometer	Xcalibur Oxford Diffraction
Radiation; λ, Å	MoK_α; 0.71073
Scan mode	ω
θ_{max}, deg	55
h, k, l ranges	$-12 < h < 12$; $-15 < k < 10$; $-23 < l < 23$
Number of measured/unique reflections with $\|F\| > 6\sigma(F)$; R_{int}, %	18528/4321; 3.4
Refinement method	Least-squares based on F
R, %	7.9
Programs	AREN [5, 6], DIFABS [7]

The Wilson statistics $|E^2 - 1|$ unambiguously indicates the absence of a centre of symmetry. Hence, the cationic moiety obtained by direct methods in sp. gr. $P\bar{1}$ was used in the automated procedure of successive approximations [6] in acentric sp. gr. $P1$ characteristic also of holotype schüllerite [3]. A complete structural model comprising 30 sites was obtained after several iterations. Due to a complex chemical composition, the cation distribution over sites was performed in accordance with the crystal-chemical criteria by analyzing the atomic displacement parameters, interatomic distances, and ionic radii of cations and was controlled by calculating the R factor. The structural model was refined by the least-squares method with the application of absorption correction [7] and using mixed atomic scattering curves for some sites. The refinement with anisotropic atomic displacement parameters based on 4321 reflections with $|F| > 6\sigma(F)$ converged to $R = 7.9\%$. All calculations were carried out with the use of the AREN program package [5, 6]. The atomic coordinates are given in Table 2. The characteristics of the coordination polyhedra are presented in Table 3.

The rather high R-factor value is attributed to the poor quality of the crystal and its mosaicity (the presence of microblocks), which is apparently associated with the presence of regions with disordered displacements of the layers. The latter fact is confirmed by the analysis of the X-ray diffraction pattern, which shows an insignificant number of reflections assigned to disordered, polytype, or hybrid structures having an increased parameter c (~30 Å), with the metric of the parameters a (~5.4 Å) and b (~7.0 Å) being unchanged. Such defects have been observed earlier in minerals of the heterophyllosilicate family [8], but they have not been found previously in lamprophyllite-group minerals.

STRUCTURE DESCRIPTION, RESULTS, AND DISCUSSION

Like in the schüllerite structure, the $A1$ and $A2$ sites located between the modules in the mineral under consideration are occupied with large Ba cations along with small amounts of K and Sr cations. These cations are located in 11-vertex polyhedra and account, in sum, for two atoms per unit cell. The distribution of the cations in the $M1$- and $M2$ five-vertex polyhedra corresponds to the Ti content similar to that observed in most of lamprophyllite-group minerals (in ericssonite and ferroericssonite, Ti is replaced by Fe^{3+}). Both sites are occupied mainly by titanium, but one site is made heavier due to the presence of iron and niobium; the other site includes an additive of lighter aluminum. However, the compositions of some octahedral sites of the O layer in the new mineral differ from those in the structure of schüllerite from the Lohley quarry. One of these sites (the $M5$ site), like that in schüllerite, is occupied by iron atoms and contains magnesium as well, with the latter dominant in this sample. As opposed to schüllerite, the $M6$ site in the new mineral is completely occupied by iron atoms. The sodium deficiency in the specimen from Kahlenberg resulted in the sodium site $M3$ being additionally occupied by

Table 2. Atomic coordinates and equivalent atomic displacement parameters (B_{eq})

Site	*x/a*	*y/b*	*z/c*	B_{eq}, Å^2
*A*1	0.0017(1)	0.9985(1)	0.0331(1)	1.24(2)
*A*2	0.4588(1)	0.4659(1)	0.9003(1)	0.85(2)
*M*1	0.0480(2)	0.5332(2)	0.1769(1)	0.74(2)
*M*2	0.4133(4)	0.9301(3)	0.7584(2)	0.79(2)
*M*3	0.4858(6)	0.6236(5)	0.4667(3)	0.76(5)
*M*4	0.9820(3)	0.8661(2)	0.4661(1)	0.84(2)
*M*5	0.4760(6)	0.1260(4)	0.4696(3)	1.23(3)
*M*6	0.9844(3)	0.3644(2)	0.4656(1)	1.13(2)
Si1	0.9095(5)	0.2008(5)	0.7385(3)	1.06(7)
Si2	0.5545(4)	0.8138(4)	0.1927(3)	0.74(7)
Si3	0.5541(5)	0.2641(5)	0.1925(3)	0.68(7)
Si4	0.9111(6)	0.6520(5)	0.7373(3)	0.88(7)
O1	0.778(1)	0.333(1)	0.124(1)	1.2(3)
O2	0.683(2)	0.134(2)	0.812(1)	1.3(3)
O3	0.685(1)	0.757(1)	0.810(1)	0.9(3)
O4	0.282(1)	0.710(1)	0.125(1)	1.0(3)
O5	0.175(1)	0.129(1)	0.813(1)	0.9(3)
O6	0.170(2)	0.752(2)	0.810(2)	1.5(3)
O7	0.282(2)	0.326(2)	0.126(1)	1.5(3)
O8	0.533(1)	0.030(1)	0.145(1)	0.9(2)
O9	0.915(3)	0.447(2)	0.803(1)	2.7(3)
O10	0.781(2)	0.716(2)	0.130(1)	2.0(2)
O11*	0.116(3)	0.076(3)	0.351(1)	1.9(3)
O12	0.103(2)	0.563(2)	0.350(1)	1.2(3)
O13	0.861(3)	0.141(2)	0.579(1)	1.8(3)
O14	0.604(2)	0.825(2)	0.351(1)	2.0(3)
O15	0.868(2)	0.619(2)	0.578(1)	1.2(3)
O16	0.614(2)	0.315(2)	0.350(1)	1.6(3)
O17	0.351(2)	0.881(2)	0.575(1)	2.0(3)
F	0.348(3)	0.363(2)	0.582(1)	1.83(7)

* The composition of the site is (O,F).

calcium, but most calcium atoms occupy the *M*4 site in equal parts with manganese atoms.

The crystal-chemical formula of Fe-schüllerite ($Z = 1$) is $(Ba_{1.6}Sr_{0.3}K_{0.1})^{XI}[(Fe^{2+},Fe^{3+})_{1.0}(Mg_{0.6}Fe^{2+}_{0.4})(Ca_{0.5}Mn_{0.5})(Na_{0.85}Ca_{0.15})]^{VI}[(Ti_{0.8}Al_{0.2})(Ti_{0.6}Fe^{3+}_{0.3}Nb_{0.1})]^{V}[Si_2O_7]_2O_2(O,F)F$, where the coordination numbers of the atoms are written as Roman numerals and the compositions of the sites located between the modules, the octahedral layer, the five-vertex polyhedra, and the diortho groups are enclosed in brackets. The idealized formula can be written as follows: $Ba_2Na(Ca,Mn)(Fe^{2+},Fe^{3+})MgTi_2[Si_2O_7]_2O_2(O,F)F$. As opposed to holotype schüllerite, in which trivalent iron predominates over divalent iron, the reverse ratio of these ions in the new mineral can be assumed based on the larger sizes of Fe-containing octahedra. Thus, the average *M*5–O and *M*6–O distances are 2.160 and 2.169 Å, respectively, in schüllerite found at the Lohley quarry and 2.22 and 2.18 Å in the specimen from Kahlenberg.

The end members of barium minerals belonging to the lamprophyllite- and schüllerite-structure types are summarized in Table 4. Two polytypes are known for lamprophyllite-group minerals which differ in the mutual arrangement of *HOH* modules: monoclinic (2*M*) and orthorhombic (2*O*). Fe-schüllerite and schüllerite are the only representatives of this group with triclinic symmetry.

All minerals listed in Table 4, except for both schüllerite samples, are characterized also by the same topology of the *HOH* module. In minerals belonging to the lamprophyllite-structure type, the diortho groups of the *H* networks face each other (Fig. 1a), whereas the *H* networks in schüllerite are shifted with respect to the *O* layer (Fig. 1b).

Since the diortho group $[Si_2O_7]$ is linked to edges of the polyhedra located between the modules and of the *O* layer, the topology of the *HOH* modules depends on the composition of the minerals and primarily on the size ratios of the cations in the *O* layer and those located between the modules. In Ba-containing min-

Table 3. Characteristics of the coordination polyhedra (Si tetrahedra are not included)

Site	Composition ($Z = 1$)	Coordination number	Cation–anion distances, Å		
			Minimum	Maximum	Average
*A*1	$Ba_{1.0}$	11	2.690(1)	3.140(1)	2.854
*A*2	$Ba_{0.6}Sr_{0.3}K_{0.1}$	11	2.710(1)	3.150(1)	2.869
*M*1	$Ti_{0.6}Fe^{3+}_{0.3}Nb_{0.1}$	5	1.710(1)	1.980(1)	1.922
*M*2	$Ti_{0.8}Al_{0.2}$	5	1.800(1)	2.000(1)	1.947
*M*3	$Na_{0.85}Ca_{0.15}$	6	2.15(1)	2.51(1)	2.27
*M*4	$Ca_{0.5}Mn_{0.5}$	6	2.10(1)	2.40(1)	2.25
*M*5	$Mg_{0.6}Fe^{2+}_{0.4}$	6	2.03(1)	2.45(1)	2.22
*M*6	$(Fe^{2+},Fe^{3+})_{1.0}$	6	2.08(1)	2.37(1)	2.18

Table 4. Chemical composition and symmetry of barium-containing minerals belonging to the lamprophyllite- and schüllerite-structure types

Mineral	Idealized formulas	Sp. gr.	References
Nabalamprophyllite	$(BaNa)Na_3Ti_3(Si_2O_7)_2O_2(OH)_2$	*P*2/*m*	[9]
Barytolamprophyllite	$Ba_2Na_3Ti_3(Si_2O_7)_2O_3(OH)$	*C*2/*m*	[10]
Emmerichite	$Ba_2Na(Na,Fe^{2+})_2Fe^{3+}Ti_2(Si_2O_7)_2O_2F_2$	*C*2/*m*	[11]
Lileyite	$Ba_2Na(Na,Fe^{2+})_2MgTi_2(Si_2O_7)_2O_2F_2$	*C*2/*m*	[12]
Schüllerite	$Ba_2Na(Mn^{2+},Ca)(Fe^{3+},Mg,Fe^{2+})_2Ti_2(Si_2O_7)_2O_2(O,F)_2$	*P*1	[4]
Fe-schüllerite	$Ba_2Na(Ca,Mn)(Fe^{2+},Fe^{3+})MgTi_2(Si_2O_7)_2O_2(O,F)F$	*P*1	Present study
Ericssonite	$Ba_2Mn_4^{2+}Fe_2^{3+}(Si_2O_7)_2O_2(OH)_2$	*C*2/*m*	[13]
Ferroericssonite	$Ba_2Fe_4^{2+}Fe_2^{3+}(Si_2O_7)_2O_2(OH)_2$	*Pnmn*	[14]

The minerals are arranged in order of decreasing sodium content.

erals of the lamprophyllite group, in which the largest Ba cations are located between the modules and smaller cations (among which sodium is the largest one) are present in the *O* layer, the topology of the *HOH* modules directly depends on the sodium content.

Three distributions of octahedra in the *O* layer can be distinguished depending on the composition of the minerals of this group. In sodium-free ericssonite and ferroericssonite, the *O* layer consists of like ribbons running along the *b* axis: Mn–Mn–Mn–Mn... and Fe–Fe–Fe–Fe..., respectively. In minerals with the maximum Na content, the octahedra are arranged in sodium ribbons Na–Na–Na–Na... alternating with ribbons with a mixed composition. Thus, in the lamprophyllite structure, the composition of the mixed ribbon is Na–Ti–Na–Ti... and lileyite contains mixed Na–Mg–Na–Mg... ribbons. The intermediate situation is observed in schüllerite from Lohley, which is characterized by the lowest Na content and in which Na–Fe^{3+}–Na–Fe^{3+}... ribbons alternate with Mn–Fe^{2+}–Mn–Fe^{2+}... ribbons. In Fe-schüllerite, both ribbons are also mixed but have different compositions (Fig. 2): Na–Mg–Na–Mg... and Ca–Fe^{2+}–Ca–Fe^{2+} (or Mn–Fe^{2+}–Mn–Fe^{2+}).

As was shown in [15], the Si_2O_7 group is the main silicate unit in compounds with large cations, because its length (4–4.2 Å) is comparable with the length of the edge of the Ca(Na) octahedron and the Si–O–Si angle is close to 180°. In lamprophyllite-group minerals, (Si_2O_7)-groups share edges with larger Ba polyhedra located between the modules, resulting in their distortion. Thus, one edge of the prism, in which the diortho group is incorporated, is elongated, whereas the other edge is shortened and is comparable with the edge of the octahedra of small cations belonging to the *O* layer; the Si–O–Si angle decreases to 140°. There-

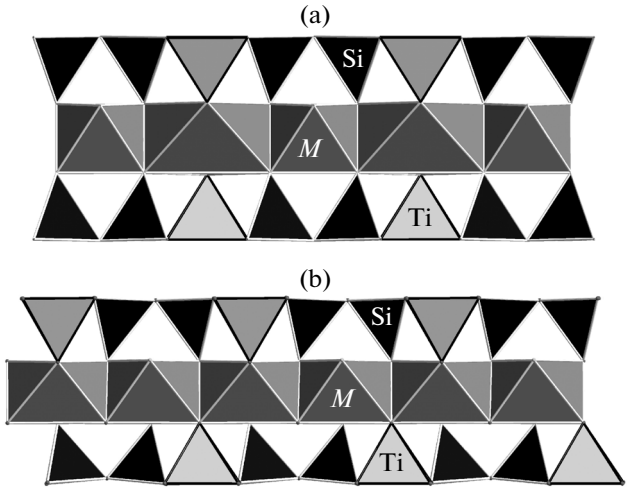

Fig. 1. Topology of the *HOH* module in minerals belonging to the (a) lamprophyllite- and (b) schüllerite-structure types.

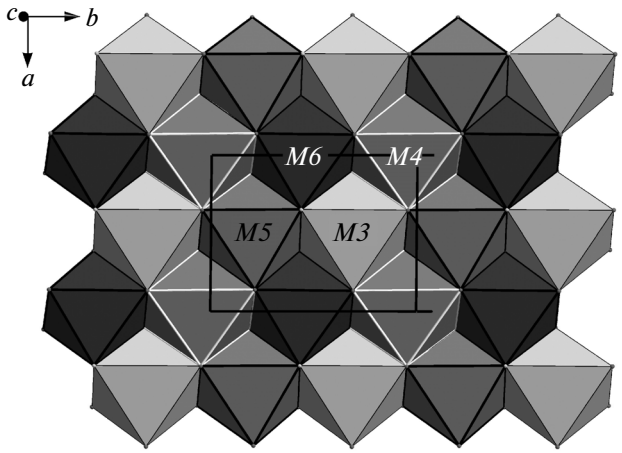

Fig. 2. Distribution of cations in octahedra of the *O* layer in the Fe-schüllerite structure.

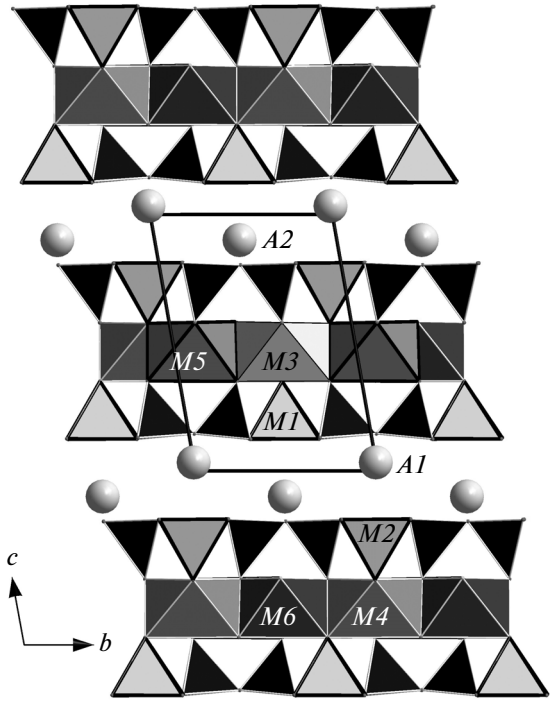

Fig. 3. General view of the Fe-schüllerite structure; *A* and *M* are cation sites.

fore, the diortho groups in lamprophyllite are forced to lean against the edges of the only small octahedron of the *M* cation (Ti). The topology of the *HOH* module remains unchanged after the replacement of Ti for other small cations (Mg in lileyite and Fe in emmerichite). The same topology of the *HOH* module is observed in sodium-free ericssonites, in which all octahedra are small. In schullerite with a complex composition, large Na octahedra are isolated and the (Si_2O_7)-groups lei against the smallest octahedra of adjacent ribbons with a shift relative to each other, resulting in a change in the topology of the *HOH* module.

Therefore, the presence of sodium in an amount of about one atom per formula unit leads to a change in the topology of the *HOH* module. The second discovery of schüllerite confirms this observation. By contrast, at a higher sodium content (more than 1.5 atoms per formula unit) the topology is the same as that observed in sodium-free minerals of the lamprophyllite group. In addition, the sodium content is an indication of the transition from lileyite to emmerichite and barytolamprophyllite. Thus, in case of the replacement of Mg by Fe^{3+} and Ti, the excessive positive charge is compensated mainly by the replacement of divalent cations with sodium, as well as of fluorine with oxygen. At even higher sodium content, excess sodium cations are located between the modules up to the domination of this element in one of the two sites between the modules in nabalamprophyllite.

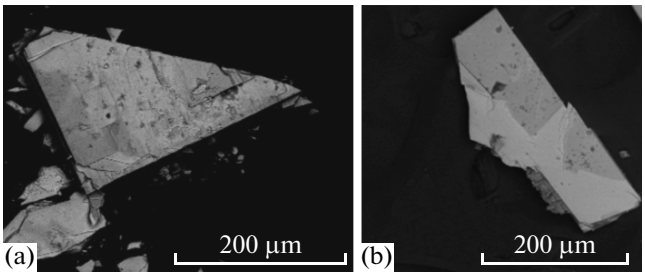

Fig. 4. Regular intergrowths of lileyite (dark areas) and schüllerite (according to the results of the study [4]). A backscattered electron image.

The fact that the unit cell parameters of schüllerite are comparable with those of lamprophyllite-group minerals is a prerequisite for the formation of their epitaxial intergrowths and mixed-layer structures. Actually, the holotype of schüllerite found at the Löhley basalt quarry was described [4] in association with epitaxial intergrowths of schullerite and lileyite. In [4] the latter was interpreted as a low-titanium barytolamprophyllite, because the existence of lileyite as an individual mineral species with a Mg-dominant octahedral site had not been established by that time. Typical intergrowths of schüllerite and lileyite are shown in Fig. 4. It can be seen that the boundaries between these two minerals can be either clear-cut or fuzzy. A similar pattern was observed in some crystals in association with schüllerite from the Kahlenberg quarry, where the crystal under consideration was found. An example of epitaxial intergrowth is displayed in Fig. 5. The numerals in Fig. 5 correspond to the numbers of microprobe analyses presented in Table 5. Point *2* corresponds to the empirical formula of lileyite $(Ba_{1.2}Sr_{0.3}K_{0.3})Na(Na_{1.1}Fe_{0.4}Ca_{0.3}Mn_{0.2})(Mg_{0.5}Ti_{0.4}Nb_{0.1})Ti_{1.9}[(Si_{3.9}Al_{0.1})O_{14}]O_{2.6}F_{1.4}$; point *5* corresponds to the formula of schüllerite

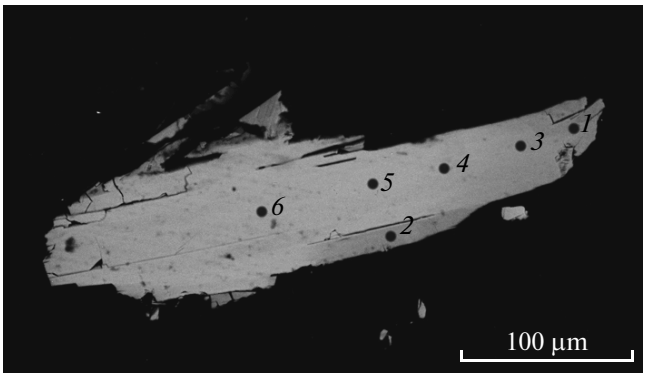

Fig. 5. Fragment of the schüllerite crystal (points *5* and *6*) with the outer zone of lileyite (points *1* and *2*) and the transition zone (points *3* and *4*). A backscattered electron image.

Table 5. Chemical composition of the schüllerite crystal shown in Fig. 5

Component	Points of analyses shown in Fig. 5					
	1	*2*	*3*	*4*	*5*	*6*
Content (wt %)						
Na_2O	7.74	7.87	6.94	5.31	4.69	4.29
K_2O	1.16	1.53	1.03	0.61	0.33	0.35
CaO	1.81	1.50	1.99	2.16	2.51	2.16
SrO	3.15	3.43	3.00	2.57	2.20	2.90
BaO	23.59	21.29	25.45	26.96	27.92	25.37
MgO	2.47	2.37	2.90	3.15	2.86	2.69
FeO	4.25	3.49	4.86	8.76	13.84	14.47
MnO	1.75	1.60	1.78	2.27	2.42	2.73
Al_2O_3	0.23	0.34	0.19	0.42	–	0.51
SiO_2	27.62	28.34	27.38	26.31	25.83	26.96
TiO_2	21.71	21.58	19.97	16.44	13.43	12.85
Nb_2O_5	0.56	1.09	–	–	–	–
F	2.84	3.08	2.79	3.79	3.11	3.43
Sum	98.88	97.51	98.28	98.75	99.14	98.71
Formula coefficients per 4(Si + Al)						
Na	2.15	2.12	1.95	1.54	1.41	1.21
K	0.21	0.27	0.19	0.12	0.06	0.06
Ca	0.28	0.22	0.31	0.35	0.42	0.34
Sr	0.26	0.28	0.25	0.22	0.20	0.24
Ba	1.33	1.16	1.45	1.58	1.69	1.44
Mg	0.53	0.49	0.63	0.70	0.66	0.58
Fe	0.51	0.41	0.59	1.09	1.79	1.76
Mn	0.21	0.19	0.22	0.29	0.32	0.34
Al	0.04	0.06	0.03	0.07	–	0.09
Si	3.96	3.94	3.97	3.93	4.00	3.91
Ti	2.34	2.26	2.18	1.84	1.56	1.40
Nb	0.04	0.07	–	–	–	–
F	1.29	1.35	1.28	1.79	1.52	1.58

Dashes indicate that the content of the component is lower than the limit of detection by electron microprobe analysis.

$(Ba_{1.7}Sr_{0.2}K_{0.1})Na_{1.2}(Fe_{1.1}Ca_{0.4}Mn_{0.3}Na_{0.2})(Mg_{0.7}Fe_{0.3})(Ti_{1.6}Fe_{0.4})[Si_{4.0}O_{14}]O_{2.5}F_{1.5}$.

As can be seen from Fig. 5, the boundary between the Fe-schüllerite and lileyite zones in the lower part of the image is clear-cut, whereas the boundary in the right upper quadrant is fuzzy. Presumably, in the latter case the transition zone (points *3* and *4*) is composed of alternating layers of both minerals. This supposition is confirmed by the X-ray diffraction data for the schüllerite crystal studied in the present work. As was mentioned above, the X-ray diffraction data set for this crystal includes reflections corresponding to the increased parameter *c*. The alternation of the modules has been observed earlier in some minerals of the herophyllosilicate family. For instance, camaraite consists of alternating bafertisite and surkhobite modules [16], bornemanite is composed of alternating lomonosovite and rosenbuschite modules [17] or of lamprophyllite and vuonnemite modules [18], and kazanskyite and nechelyustovite are built up of alternating lamprophyllite and epistolite modules [19, 20].

CONCLUSIONS

The sodium content in lamprophyllite-group minerals can be considered an indication that a particular mineral species belongs to a certain mineral type. The assignment of schüllerite to the lamprophyllite group

is a controversial point because of the topological features of this mineral. However, schüllerite differs from heterophyllosilicates, which are characterized by *H* networks shifted with respect to each other (for example, from bafertisite), not only by the stoichiometry but also by the location of Ti in a half-octahedron (instead of an octahedron) and the presence of a Na-dominant site in the *O* layer. The topology of Fe-schüllerite (like that of schüllerite) combines (Fig. 3) their distinguishing features. On the one hand, this mineral contains five-vertex polyhedra of titanium in the *H* network. On the other hand, the diortho groups in this mineral are shifted with respect to each other in the *HOH* module. However, although the former feature is of most importance, schüllerite and its iron-rich variety can be considered in one series with lamprophyllite-group minerals.

Regular intergrowths of schüllerite and lamprophyllite-group minerals are prerequisites for the formation of a new type of hybrid structures containing schüllerite and lamprophyllite modules simultaneously.

ACKNOWLEDGMENTS

This study was supported by the Russian Foundation for Basic Research (project no. 14-05-31150-mol_a) and the Council on Grants from the President of the Russian Federation (Federal Programs on Support of Young Scientists and Leading Scientific Schools; grant nos. MK-4990.2014.5 and NSh-2150.2012.5).

REFERENCES

1. G. Ferraris and A. Gula, Rev. Mineral. Geochem. **57**, 69 (2005).
2. R. K. Rastsvetaeva and S. M. Aksenov, Crystallogr. Rep. **56** (6), 910 (2011).
3. R. K. Rastsvetaeva, S. M. Aksenov, and N. V. Chukanov, Dokl. Chem. **437** (2), 90 (2011).
4. N. V. Chukanov, R. K. Rastsvetaeva, S. N. Britvin, et al., Geol. Ore Deposits **53** (8), 767 (2011).
5. V. I. Andrianov, Kristallografiya **34** (3), 592 (1989).
6. V. I. Andrianov, Kristallografiya **32** (1), 228 (1987).
7. N. Walker and D. Stuart, Acta Crystallogr. A **39** (2), 158 (1983).
8. P. Németh, G. Ferraris, G. Radnoczi, and O. A. Ageeva, Can. Mineral. **43**, 973 (2005).
9. R. K. Rastsvetaeva and N. V. Chukanov, Dokl. Akad. Nauk **368** (4), 492 (1999).
10. Z. Z. Peng, J. Zhang, and J. Shu, Kexue Tongbao **29**, 237 (1984).
11. S. M. Aksenov, R. K. Rastsvetaeva, and N. V. Chukanov, Z. Kristallogr. **229** (2), 1 (2014).
12. N. V. Chukanov, I. V. Pekov, R. K. Rastsvetaeva, et al., Eur. J. Mineral. **24** (1), 181 (2012).
13. P. B. Moore, Lithos. **4** (2), 137 (1971).
14. S. Matsubara, Mineral J. **10** (3), 107 (1980).
15. N. V. Belov, *Crystal Chemistry of Silicates with Large Cations* (Izd-vo AN SSSR, Moscow, 1961) [in Russian].
16. F. Cámara, E. Sokolova, and F. Nieto, Mineral. Mag. **73**, 855 (2009).
17. G. Ferraris, E. Belluso, A. Gula, et al., Can. Mineral. **39**, 1665 (2001).
18. F. Cámara and E. Sokolova, Mineral. Mag. **71**, 593 (2007).
19. F. Cámara, E. Sokolova, and F. Hawthorne, Mineral. Mag. **76**, 473 (2012).
20. F. Cámara and E. Sokolova, Mineral. Mag. **73**, 887 (2009).

Translated by T. Safonova